

**NASA TECHNICAL
MEMORANDUM**

NASA TM X-71654

NASA TM X-71654

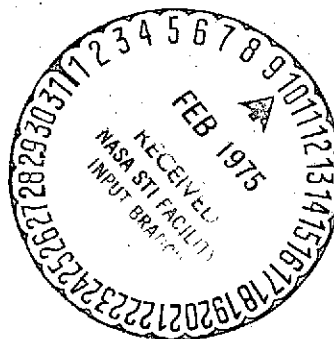
(NASA-TM-X-71654) STUDIES OF INTERNAL
SPUTTERING IN A 30-cm ION THRUSTER (NASA)
14 p HC \$3.25 CSCL 21C

N75-15736

Unclas
G3/20 07777

**STUDIES OF INTERNAL SPUTTERING
IN A 30-CM ION THRUSTER**

M. A. Mantenicks and V. K. Rawlin
Lewis Research Center
Cleveland, Ohio 44135



TECHNICAL PAPER to be presented at
Eleventh Electric Propulsion Conference sponsored
by American Institute of Aeronautics and Astronautics
New Orleans, Louisiana, March 19-21, 1975

STUDIES OF INTERNAL SPUTTERING IN A 30-CM ION THRUSTER

M. A. Mantenicks and V. K. Rawlin
Lewis Research Center
National Aeronautics and Space Administration
Cleveland, Ohio

Abstract

Initial studies have been made of the sputtering and deposition phenomena in a 30-cm thruster. Sputtering rates, of the cathode baffle, one of the main sources of sputtered material in a thruster, have been measured by weight loss as a function of several thruster parameters. Sputtering rates were found to increase with both cathode flow rate and beam current when constant discharge voltage of 37 volts and power losses of 185 ev/ion were maintained. Sputtering rates were reduced 24% as discharge voltage was decreased from 37 to 33 volts while keeping discharge power constant. Qualitative agreement was found between sputtering rates obtained by the weight loss and those implied by spectroscopically observed line intensities of the excited iron sputtered atoms. After the completion of the sputtering tests, deposition and sputtering sites inside the thruster were identified.

I. Introduction

Long term ion thruster and component tests have indicated that sputtering damage of thruster internal components can occur and may be minimized if certain precautions, such as proper choice of materials, geometries, and operating conditions are taken. (1)(2)(3) As evidenced by the Hughes R. L. life test (4) initial precautions reduced internal sputtering sufficiently to ensure thruster performance for time period of about eight months. After this time cathode baffle erosion was found in the test. This erosion while not preventing ongoing thruster operation, can be expected over longer time periods to result in thruster control problems. Life tests have also revealed that an equally important aspect of the sputtering problem is the adhesion characteristics of the sputtered material on thruster component surfaces. Spalling of deposited layers may short insulators and/or cause grid shorting and subsequent grid damage as observed in the Hughes R.L. life test. It is therefore, of utmost importance to understand the sputtering-deposition process inside a thruster to insure very long life time thruster operation. A thorough sputter erosion study has been performed for the 5-cm thruster components at three discharge voltage conditions. (5) Additional work has been performed with the 5-cm thruster to study the adherence characteristics of the sputtered material on different surfaces. (6) In reference 6 sputtering rates were found to increase with increasing discharge voltage and superior adhesion to grit-blasted and screen surfaces of deposited sputtered material also were observed.

This paper describes the sputtering-deposition phenomenon observed in a 30-cm diameter Hg ion thruster. Sputtering rates of a typical heavily eroded thruster component, the cathode baffle, were obtained in short duration tests (50-150 hours) and are presented as a function of thruster parameters such as cathode mass flow rate, magnetic baffle current, discharge voltage, ion beam current, and

discharge fluctuations. Because of its easy accessibility and simple geometry the baffle lends itself to quick and convenient sputtering rate measurements. Different baffle geometries and materials were also tested. Sputtering rates obtained by weight loss were correlated with iron spectral line intensities measured in the thruster discharge. Spectroscopic methods of studying sputtering have been employed by Stuart and Wehner to measure sputtering rates at low ion energies (7) and ideally the line intensity should correlate directly to the sputtering rate.

After the sputtering tests were concluded, the thruster was examined to determine the deposition and/or sputtering sites. Chemical analyses were made of the deposits in order to determine their origin. Scanning electron microscope pictures of some of the deposited layers were taken.

II. Apparatus and Procedure

A "400 series" thruster (8) modified to have the same discharge chamber performance characteristics as the Engineering Model Thruster (EMT) (9) was used for the sputtering experiments. Figure 1 shows a cross-sectional view of the thruster with its components. The cathode assembly was modified to conform to the EMT geometry by shortening the cathode tip to baffle distance by 2.54-cm. The magnetic baffle used a 3-1/2 turn coil. The "700 series" EMT used in the Hughes R.L. life test (4) differs from the Lewis Research Center's modified "400 series" thruster by having a separated cathode-isolator-isolator (C-IV) and its different cathode baffle mount (Fig. 2).

Table I lists the different thruster operating conditions used in the sputtering tests. Also listed are the sizes and materials of the different cathode baffles used in each test. Two layer baffles were used to separate upstream (cathode side) and downstream (anode side) weight changes. The baffle geometries used are shown in Figure 3.

The perforated baffles had four (0.635 diam.) stainless steel screen covered holes. A baffle used to measure the erosion profile across its diameter was made by placing thin (0.127 mm) Ta masks on both sides of a mirror polished mild steel baffle. Each mask had four 3.18 mm holes located on three radii as shown in Figure 3. A well defined sputtered or deposited region was formed on the exposed circular areas of the mild steel baffle during the test. Afterwards these areas were scanned with a profileometer.

The thruster was operated in a 3.05 m diameter port of a 7.6 m diameter x 21.4 m long vacuum facility. Use of the large tank minimized the backsputtered material from the tank. The pressure in the tank during thruster operation was in the low 10^{-6} torr range. The thruster was operated at constant thruster parameters by the use of three vaporizer control loops. The "standard"

thruster operating conditions of a 30-cm thruster were discharge voltage (ΔV_I) 37 volts, discharge emission current (JE) 10 amps, screen voltage (V_I) 1100 volts, accelerator voltage (V_A) 500 volts, beam current (J_B) 2.0 amps, cathode equivalent flow rate (J_{OK}) \sim 80 ma, keeper voltage (V_{CK}) \sim 6 volts, keeper current (J_{CK}) 0.5 amps.

A 1.5 m Jarrell Ash spectrometer was used to observe the spectral intensities of iron (3720Å) and Mo (3864Å) atomic emission lines. The spectrometer was located at the opposite end of the tank and viewed the thruster through a quartz window.

III. Results and Discussion

Sputtering Rates of the Cathode Baffle

Sputtering rates per unit area for a given material in a thruster should depend on the current density and energy of the mercury ions arriving at the surface. For low energy ions the sputter yield is proportional to $(E - E_0)^3$ (10) where E is the ion energy and E_0 is the threshold energy of the sputtered material. Also, for low ion energies found inside the thruster the angle of incidence of the ions should not be a factor in the sputtering rates. (11)

An equation, taking into account the presence of double ions, but neglecting triple ions, can be derived to give an approximate sputtering rate.

$$M = \frac{I_T A}{10^5} \left[S_+ + \frac{i_2}{2I_T} (S_{++} - 2S_+) \right] \quad (1)$$

where

M	mass loss rate, gm/sec
A	atomic weight of sputtered material, Amu
i_1	Hg ⁺¹ ion current to sputtered surface, amp
i_2	Hg ⁺² ion current to sputtered surface, amp
I_T	total ($i_1 + i_2$) ion current to sputtered surface, amp
S_+	sputter yield of incident ion (atoms/ion)
S_{++}	sputter yield of incident double ion (atoms/ion)

Sputter yields at low energies are difficult to obtain and the existing literature in this area is very limited. For the calculations in the present work the results of Askerov and Sena for mercury ions on iron (10) were used.

Effects of cathode mass flow rate, baffle diameter and magnetic baffle current. Figure 4 shows the sputtering rate (M_{total}) of the baffle as a function of the cathode flow rate J_{OK} for three baffle diameters for a thruster operated at 2.0 amp beam current J_B , 37.0 volt discharge voltage ΔV_I and 10.0 amp emission current JE. The cathode flow rate J_{MB} was varied by changing the magnetic baffle current while discharge conditions were held constant. The magnetic baffle current is given for each data point in the figure.

For all three baffle diameters the total baffle sputtering rate increases with cathode flow rate. The absolute magnitude and sensitivity of the sputtering rates increased with increasing baffle diameter.

Figure 5 separates the wear rates for the up-

stream and downstream baffles as determined from the experiment with the multi-layered baffles when one or more layers were tested. The wear rates for the upstream side of the baffle were always less than those for the downstream side and were nearly independent of the cathode flow rate and baffle diameter. The measured weight loss rates ranged for the downstream side of the 5.72-cm baffle, from 0.45 mg/hr for 80 mA cathode flow rate to 1 mg/hr at 135 mA.

Figure 6 shows the sputtering rates per unit area of the downstream sides of the three different baffles tested. It is seen that the rates per unit area are nearly the same for all three baffle diameters, and show essentially the same increase with cathode flow rate.

An estimate of the expected sputtering rates may be obtained by Equation 1. Values of $[S_+]_{37V} = 5 \times 10^{-4}$ atoms/ion and $[S_{++}]_{37V} = [S_+]_{74V} = 9 \times 10^{-3}$ atoms/ion were used. (10) I_T was obtained from the saturated ion current of an electrically isolated baffle. The saturated total ion current I_T , to only the downstream surface of the 5.72-cm diameter baffle, with a discharge voltage at 37 volts and a 2 amp beam current, was measured to be 0.14 amps. A ratio of $[i_2/i_1]_{37V} = 0.45$ was used, which was estimated from double ion measurements on the center line outside the thruster (12) for similar thruster conditions to those in the experiments reported here. A sputtering rate of 0.5 mg/hr is predicted by Equation 1 for the downstream side of the baffle. Assuming a uniform sputtering rate across the downstream side of the baffle, this rate represents a 2.5×10^{-2} -cm thickness loss for a 5.72-cm diameter baffle in 10,000 hours. This calculation agrees with the measured loss rate of the downstream baffle at the low cathode flow rate but is considerably lower than the average erosion rate of approximately 1.3×10^{-1} -cm/10,000 hours found in the center of the baffle in life test reported in reference 4.

Variation of the magnetic baffle current does not of itself strongly impact the baffle sputtering rate. This may be seen from Figure 4 where little effect on the sputtering rates was indicated for large changes of magnetic baffle current. Even though the total sputtering rate may not be affected by the magnetic baffle current, it is likely that the plasma density profiles in the baffle region are significantly altered by varying the magnetic field there via changes in J_{MB} . Such changes in the plasma density profiles could result in different sputtering profiles across the baffle diameter.

The increase noted in the sputtering rate of the baffle downstream surface with increasing cathode mass flow rate is probably associated with increasing ion production rates. This explanation is consistent with the increase in the saturated ion current to the baffle's downstream surface observed on increasing cathode mass flow rate.

The sputtering observed on the upstream side of the baffle is not entirely understood because for single and doubly charged ions the ion energies in this region should be below the sputtering threshold energies of the baffle material.

It should be noted that sputtering is kept to a minimum at the low cathode flow rates where the

thruster operates most efficiently. (13)

Discharge voltage. Figure 7 shows the sputtering rates of a single layer mild steel baffle as a function of discharge voltage at constant discharge power and a 2 amp beam current. Decreasing the discharge voltage from 37 to 33 volts resulted in a 24% decrease in sputtering rate. Again Equation 1 may be used to calculate the expected decrease. Sputter yields of $[S_+]_{33V} = 3 \times 10^{-4}$ and $[S_+]_{66V} = [S_+]_{33V} = 5 \times 10^{-3}$ (10) and $(I_2/I_1)_{33V} = 0.35$ (12) were used. The total saturated ion current measured at 33 volts was 0.19 amps. The calculated decrease of the sputtering rate is 32% which is in fair agreement with the measured weight change. Therefore, it appears that reduction of discharge voltage (at constant discharge power) will not reduce sputtering rates appreciably at a beam current of 2 amps. This result does not necessarily contradict the conclusions of reference 5 where a stronger dependence of discharge voltage on sputtering rates was found. The different behavior of the two thrusters may be accounted for in the differences of the primary electron energies in the two thrusters. The primary electron energy (V_p) may be estimated by $\Delta V_I - V_{Ck}$. The approximate values of these energies is about 31 volts and 23 volts for the large and small thrusters, respectively. The double ion production rate is more sensitive to the primary electron energy at the lower electron energy levels than at the higher levels. (5) Therefore, less dependence of sputtering rates on discharge voltage may be expected for the 30-cm thruster at the 2 amp beam condition than the 5-cm thruster.

Beam current. Figure 8 shows the downstream and upstream baffle surface sputtering rates for a two to one variation in ion beam current at constant ev/ion. Also shown are comparable data for throttled thruster operation at two increased discharge voltage conditions. The sputtering rate for the downstream side of the baffle decreases with decreasing beam current even though the cathode flow rate is slightly higher for the lowest (1.0A) beam condition. These observations are reasonable in view of the increases in the Hg^+ and Hg^{++} ion density which occur in the discharge chamber with increasing total Hg flow rate and discharge power required for the increased ion beam current. The difference in sputtering rates at the lower beam conditions at the different discharge voltages are larger than at the previously discussed condition of 2.0 amp beam current. This difference may be explained again by a relatively larger difference of the primary electron energy and the lower level of the 37 volt case at the 1.0 amp beam level. The values of V_p were 28 and 32 volts at ΔV_I 's of 37 and 42 volts respectively.

The rates, however, are again relatively constant for the upstream side of the baffle. Also the sputtering rates of the upstream side of the baffle were not affected appreciably by the increased discharge voltage conditions.

Discharge fluctuations. It is possible that fluctuations in the discharge may influence the sputtering rates of thruster components. RMS values of discharge voltage and current fluctuations were measured for various baffle sizes. Figure 9 shows a typical discharge fluctuation

characteristic for a 2 layer iron 5.08-cm baffle. (14) The fluctuations tend to increase with increasing cathode mass flow rate but do not, however, follow the linear relationship with cathode flow rate exhibited by the sputtering rate.

Materials. Sputtering rates of thruster components may be reduced if materials are chosen for them which have a lower sputter yield and are compatible with the thruster environment. Iron, which the cathode baffle and pole piece are made of, cannot be readily replaced because of the required magnetic circuit. But these two components may be coated or shielded with lower sputter yield materials. Molybdenum and carbon are possible choices if coating techniques are available which provide good bonding of them to iron.

Experiments with a tantalum shielded baffle were performed, since tantalum is easily coated on an iron surface. The tantalum proved to have a 2 to 4 times lower mass sputtering rate than iron at the low cathode flow rate (Fig. 6) and showed even greater improvement at the higher cathode mass flow rates. Sputtering rates found in literature do not agree with the lower measured rates in the thruster. At this time the discrepancy is not understood.

Beam-off operation. The sputtering rates during beam-off operation, such as during thruster warm-up intervals, may be important, and hence experiments were performed to determine these rates. It was found by weight loss that sputtering rate of the baffle was ~6 times less for a Ta baffle for thruster operation without beam extraction at a 2.0 amp main flow rate than with a beam on. This may be due to the effect of the higher pressure inside the discharge chamber, which would lower the electron temperature and therefore decrease the ion production rate.

Baffle Sputtering Profile

The previous weight measurements would be more useful if the distribution of the sputtering erosion across the baffle diameter were known. Therefore a polished masked mild steel baffle was tested at a 2 amp beam current and a cathode flow rate of 155 mA (higher than standard). The results show in Figure 10 that the sputtering was found to be greatest in the central region of the downstream side of the baffle. This behavior was also observed in the life test (4) where a hole in the center of the baffle first appeared. The upstream side of the baffle on the other hand had accumulated about a 1 to 2 micron thick deposit in the 75 hours test. However, on the very center of the upstream side of the baffle both deposition and sputtering were found with 7.5 micron deep narrow pits and 12 micron peaks. Profileometer traces of the baffle surfaces are seen in Figure 11. Some focused sputtering effects observed here on the downstream side may have been due to possible separation of the mask from the baffle surface or to other mechanisms involving the mask hole edges. The integrated sputter rate based on the measured erosion depth of the center sputtered region on the downstream surface is 0.81 mg/hr. This is about 15% higher than the extrapolated erosion rate for the 5.08-cm baffle obtained from Figure 5. The observed deposit on the upstream side of the baffle

may not be typical since mass loss has been measured of the downstream side in the previously described data. It is probable that the upstream side may undergo sputtering in the center region of the baffle and deposition on the outer areas. However, it appears that sputtering erosion is still less at the upstream side except for the very center of the baffle than at the downstream side of the baffle.

Spectroscopic Measurements

Spectroscopic methods of studying sputtering has been employed by Stuart and Wehner⁽⁷⁾ to measure sputtering rates at low ion energies. They found that the sputtered atoms from a clean metal surface are mostly ejected in a neutral, unexcited state, but will undergo excitation in the plasma. Hence such atoms will be excited by the plasma in an ion thruster. It is therefore possible to observe the atomic emission spectrum of the sputtered atoms superimposed on the emission spectrum of the mercury vapor in an ion thruster discharge. The intensity of the sputtered atom spectral lines is proportional to the density of the sputtered atoms in the region of the discharge. By assuming that the density of the sputtered atoms in the discharge is proportional to their sputtering rate, the observed intensities of the spectral lines are therefore proportional to the sputtering rates. In order for these assumptions to hold, however, the discharge conditions must be kept constant. There appears to be no interference to the atomic emission lines from the beam outside the thruster.⁽¹⁵⁾ Figure 12 shows the spectral intensity of the iron line (3720 Å) observed as a function of magnetic baffle current for a 4.76-cm diameter iron baffle at three discharge voltages. (Cathode flow rates were not measured during the spectroscopic tests as only short term tests were conducted in order to keep window contamination to a minimum). A relative increase of 32% was observed of the iron intensity at 37 volts ΔV_I over a magnetic baffle current range from 14 to 20 amps. The corresponding relative increase in the measured weight loss rates, from Figure 4 for the same baffle size and a similar change in magnetic baffle current is 36%. The spectroscopic intensities also indicate less dependence of sputtering rates with J_{MB} at lower discharge voltages.

Figure 13 represents relative changes of the iron line intensity from the "standard" thruster operating conditions observed as a function of different thruster parameters for a thruster with a 5.7-cm diameter iron baffle sandwiched by tantalum discs. In this test, as before, the observed iron line intensity should correspond to the total sputtering rate of the exposed iron and steel components subject to sputtering. This total sputtering rate should approximately duplicate the trends found earlier in the measured sputter erosion rate of the iron baffle.⁽⁵⁾ The iron intensity was found to decrease 45% as the beam current was decreased from 2.0 to 1.0 amp. This change agrees with that observed in the corresponding measured weight losses observed before as shown in Figure 8. The iron intensity increased approximately 30% as the discharge voltage was increased from 35.7 to 39.8 volts. About the same increase was noted before (see Fig. 7) between the baffle erosion rates measured at 33 and 37 volts ΔV_I . Also the iron intensity increased by 20% for

magnetic baffle current increase of 0 to 5 amps. The sputtering rate increase for a corresponding increase in J_{OK} (from 125 to 160 ma) obtained from the slope of the line in Figure 6 is 25%. Thus it appears that qualitative agreement was found between sputtering rates measured by weight loss and those implied by spectroscopically observed line intensities of the excited sputtered atoms for such thruster parameters as cathode flow rate and ion beam current.

Some measurements were also made of the Mo line (3864 Å) intensity observed in the thruster discharge. These indicated that the Mo sputtering rate was more sensitive to discharge voltage and emission current variations than the iron spectroscopically observed sputtering rate, but less sensitive to cathode flow rate variations. The molybdenum line intensity also appeared to depend on the accelerator and screen voltages, but was not directly associated with accelerator drain current variations. Thus it appears that these observations are consistent with locations of iron and molybdenum parts in the thruster. The spectroscopic line intensity measurements also confirmed the much lower sputter rates previously noted with the thruster operating without beam extraction at 2 amp main flow, but indicated higher sputtering rates with the beam off at 1 amp main flow than with the beam on. Also the spectroscopic measurements indicated considerably higher sputtering rates during short circuits between the grids, as compared to the sputtering rates indicated under normal thruster operation.

Identification of Sputtered and Deposited Thruster Components

The thruster used in the tests described earlier in this paper was closely examined following the tests to determine which components were sputtered and on which the sputtered materials had deposited. At the time of examination, the thruster body and anode had accumulated 4560 hours of operation under various conditions. The deposited coatings found were spectroscopically analyzed and were examined with a scanning electron microscope.

A summary of the results appear in Table II. The major sputtered components were the cathode baffle, cathode pole piece and the accelerator grid. The cathode baffle sputtering and deposition phenomenon have already been described. The deposits on the upstream side of the baffle were analyzed to consist of 65% Fe, 23% Ni, 7% Mo and 1.5% Cu. It is presumed that the iron came from the cathode pole piece and cathode back plate. The nickel probably derived from the original nickel plating of the mild steel parts inside the thruster. The Mo must have come from the grids. The copper may be backsputtered material from the LN₂-cooled copper liner of the tank or from two tests where copper plated cathode baffles was tested. It was estimated from micrometer measurements, that the cathode pole piece was most heavily eroded on the inside lip of the pole piece, but accurate dimensional loss measurements could not be made.

The screen grid was found to have gained a negligible amount of weight, 1.9 grams, in 1872 hours of thruster operation. A thin sputtered-deposited layer was observed upstream in the peripheral regions of the screen grid. The deposit

was analyzed to consist of 75% Mo, 20% Fe, 2% Ni, 1% Cu. The source of the iron probably is the cathode baffle and pole piece. The Mo is material sputtered from other areas of the grid system. No accurate measurement of the thickness reduction in the center of the screen grid was possible. The accelerator grid was found to have a small weight loss of 3.3 grams in 1872 hours of thruster operation.

The entire anode was found to be coated with sputtered material. A typical flake from this coating is seen as viewed with the scanning electron microscope at a magnification of 2000 (Fig. 14). The several layers which are seen on the flake edge probably represent extended periods of operation at different thruster operating conditions. A representative flake from the deposit at the downstream end of the anode was analyzed to consist of 25% Fe, 51% Mo, 9% Ta, 8% Cu, 5% Ni, 9% Cr. The Mo concentration of the anode coating was found to decrease with distance upstream from the grids. The iron concentration increases however, with distance upstream from the grids. The same trends were observed in reference 5. The copper concentration was found to increase with distance upstream from the grids. The relatively small concentration of chromium found in the anode coating indicates a low rate of arrival of material back-sputtered from the opposite end of the stainless steel tank.

Considerable deposition of sputtered material was observed to have taken place inside the cathode chamber. Components such as the insulator shadow shields of the keeper and magnetic baffle, which are at keeper and floating potentials, respectively, accumulated the thickest deposits. Flaking of the deposit on a shadow shield surface is seen in Figure 15. A typical composition of these deposits was found to be 65% Fe, 15% Ta, 14% Ni, 3% Cu and 2% Mo. The Mo keeper was found to have a coating on its upstream side, consisting of 58% Ni, 19% Fe, 19% Ta and 2% W. The thruster backplate and manifold were found to be coated with a deposit analyzed to contain 58% Mo, 15% Cu, 11% Fe, 8% Ta, 1.9% Cr. The stainless steel indicated by the iron to chromium ratio may be from back-sputtered tank material or the stainless steel base of the manifold.

Since the sputtered and deposited sites have been identified, corrective measures can be taken to ensure long term thruster operation. These include coating the surfaces subject to sputtering such as cathode baffle and pole piece, with low sputter yield materials such as Ta, Mo or graphite. To prevent spalling of sputtered coatings from surfaces on which they deposit, grit blasting the surfaces or covering them with grit blasted screens is recommended. (6)

IV. Conclusions

It is apparent that all thruster components undergo net mass change to some degree during thruster operation. A thruster component will suffer sputtering and/or deposition depending on its location, the thruster operating conditions and its electrical potential. These processes have been identified by this report and corrective solutions can be taken to ensure, reliable, long term thruster operation.

Sputtering rates of the cathode baffle, one of the main sources of sputtered material in the 30-cm thruster, have been measured as a function of the cathode flow rate, magnetic baffle current, discharge voltage (at constant discharge power), and beam current. Baffle sputtering rates were also measured as a function of baffle diameter and for both Ta and Fe baffles.

It was found that the baffle sputtering rates increased with increasing cathode flow rate for a discharge voltage of 37 volts and a 2.0 amp beam current. The erosion rate per unit area was calculated about the same for all three baffle diameters tested. Sputtering rates were reduced by 24% as the discharge voltage was decreased from 37 to 33 volts while keeping discharge power constant at the 2 amp beam condition, but greater differences were found at lower beam levels. Sputtering rates were found to decrease with decreasing beam current.

It was found that baffle sputtering rate was reduced considerably by use of Ta for the baffle surface.

Preliminary attempts at relating spectral line intensities of sputtered materials to their sputtering rates proved encouraging. Qualitative agreement was found between sputtering rates measured by the weight loss method and those implied by spectroscopically observed line intensities of the excited sputtered atoms for such thruster parameters as cathode flow rate, ion beam current.

Examination of the thruster revealed that the cathode baffle and cathode pole piece were the main source of sputtered iron. Major deposit sites included the anode, the shadow shields inside the cathode chamber, the backplate and the manifold. The screen grid was found to have gained 1.9 grams in 1872 hours, whereas the accelerator grid lost 3.3 grams in the same time period.

References

1. Kerslake, W. R., Goldman, R. G. and Nieberding, W. C., "SERT II: Mission, Thruster Performance, and in-Flight Thrust Measurements," Journal of Spacecraft and Rockets, Vol. 8, No. 3, Mar. 1971, pp. 213-224.
2. Bechtel, R. T., "Component Testing of a 30-Centimeter Diameter Electron Bombardment Thruster," AIAA Paper 70-1100, Stanford, Calif., 1970.
3. Nakanishi, S., and Finke, R. C., "9700-Hour Durability Test of a Five Centimeter Diameter Ion Thruster," Journal of Spacecraft and Rockets, Vol. 11, No. 8, Aug. 1974, pp. 560-566.
4. Collett, C. R., "A 7700-Hour Endurance Test of a 30-Centimeter Kaufman Thruster," AIAA Paper 75-366, New Orleans, La., 1975.
5. Power, J. L., "Sputter Erosion and Deposition in the Discharge Chamber of a Small Mercury Ion Thruster," AIAA Paper 73-1109, Lake Tahoe, Nev., 1973.
6. Power, J. L., "Solutions for Discharge Chamber Sputtering and Anode Deposit Spalling in Small Ion Thrusters," AIAA Paper 75-399, New Orleans, La., 1975.

7. Stuart, R. V., Wehner, G. K., "Sputtering Yields at Very Low Bombarding Ion energies," Journal of Applied Physics, Vol. 33, No. 7, July 1962, pp. 2345-2352.
8. King, H. L., and Poeschel, R. L., "Low Specific Impulse Ion Engine," Feb. 1970, Hughes Research Labs., Malibu, Calif.; also CR-72677, 1970, NASA.
9. Poeschel, R. L., King, H. J. and Schnelker, D. E., "An Engineering Model 30-cm Ion Thruster," AIAA Paper 73-1084, Lake Tahoe, Nev., 1973.
10. Askerov, Sh. G., Sena, L. A., "Cathode Sputtering of Metals by Slow Mercury Ions," Soviet Physics - Solid State, Vol. 11, No. 6, Dec. 1969, pp. 1288-1293.
11. Wehner, G., "Influence of the Angle of Incidence on Sputtering Yields," Journal of Applied Physics, Vol. 30, No. 11, Nov. 1969, pp. 1762-1765.
12. Poeschel, R. L., "A 2.5-kW Advanced Technology Ion Thruster," August 1974 Hughes Research Labs., Malibu, Calif.; also CR-134687, 1974, NASA.
13. Rawlin, V. K., "Performance of 30-Centimeter Thruster with Dished Accelerator Grids," AIAA Paper 73-1053, Lake Tahoe, Nev., 1973.
14. Serafini, J. S., Mantenieks, M. A. Rawlin, V. K., "Dynamic Characteristics of a 30-Centimeter Mercury Ion Thruster," AIAA Paper 75-345, New Orleans, La., 1975.
15. Milder, N. L., Sovei, J. S., "Optical Radiation from Regions Downstream of Mercury Bombardment Thrusters," AIAA Paper 72-441, Bethesda, Md., 1972.

TABLE I. Thruster operating conditions, baffle geometries and their sputter rates

[eV/ion = 185; V_I = 1100; and V_A = 500]

Test	Baffle diam, cm	Length of test, hr	Up-stream baffle material	Down stream baffle material	Up-stream baffle wear rate, mg/hr	Down stream baffle wear rate, mg/hr	Total wear rate, mg/hr	Cathode flow rate, mA	Magnetic baffle current, amp	Beam current, amp	Discharge voltage, V	Baffle geometry
1	5.72	48.3	Fe	Fe	0.083	0.973	1.056	132	5	2.0	37	2 layer solid
2	5.72	55.5	Fe	Fe	0.180	0.775	0.955	123	5			
3	5.72	107.1	Fe	Fe	0.065	0.456	0.521	80	2			
4	5.08	69.1	Fe	Fe	0.170	0.610	0.780	136	8.5			
5	5.08	49.0	Single	Fe	-	-	0.367	70	12			Solid
6	5.08	69.1	Single	Fe	-	-	0.420	80	12			Solid
7	4.76	68.1	Fe	Fe	0.103	0.426	0.529	120	20			2 layer solid
8		95.7	Fe	Fe	0.083	0.303	0.386	76	15			2 layer solid
9		70.9	Single	Fe	-	-	0.402	80	19			Solid
10		65.7	Single	Fe	-	-	0.312	80	17		35	Solid
11		160.9	Single	Fe	-	-	0.304	70	14		33	Solid
12	5.72	42.8	Fe	Ta	0.14	0.210	0.350	150	10		37	2 layer solid
13	5.72	102.9	Ta	Ta	0.068	0.126	0.194	76	2			3 layer solid
14	5.08	118.6	Fe	Fe	0.051	0.450	0.501	102	4			2 layer perforated
15		73.7			0.122	0.244	0.366	130	7	1.5		
16		69.9			0.072	0.314	0.386	89	6	1.5	40	
17		156.4			0.084	0.179	0.263	130	6	1.0	37	
18		91.3			0.120	0.420	0.540	106	7	1.0	42	
19		75.5	Ta (Mask)	Ta (Mask)	-	-	0.81 (EST.)	155	7	2.0	37	Fe with Ta masks

Table II. Summary of sputtered and deposited thruster components

Sputtered parts	Deposited parts	Comments
Cathode baffle	Cathode baffle	Sputtered on downstream side, deposit on upstream side except for the center of the baffle. Deposit consists of 65% Fe, 23% Ni, 8% Mo, 1.5% Cu
Cathode pole piece	Cathode pole piece	Sputtered mostly on downstream edge
	Cathode keeper	Deposit on upstream side: 58% Ni, 19% Fe, 19% Ta, 2% W
	Cathode backplate	Some deposit (visual observation)
	Manifold	Deposit from screen: 58% Mo, 15% Cu, 11% Fe, 8% Ta, 4% Al, 2% Ni, 1.9% Cr
	Backplate	Similar to manifold (visual observation)
	Anode	Deposit: 51% Mo, 25% Fe, 8% Cu, 9% Ta, 5% Ni, 0.9% Cr
	Insulator sputter shields on keeper and mag baffle	Deposit: 65% Fe, 15% Ta, 14% Ni, 3% Cu, 2% Mo
Screen grid	Screen grid	Deposit on peripheral upstream region: 75% Mo, 20% Fe, 2% Ni, 1% Cu. Sputtered in center. Net weight gained of 1.9 gr/1872 hours
Accelerator grid		Net weight lost 3.3 gr/1872 hours

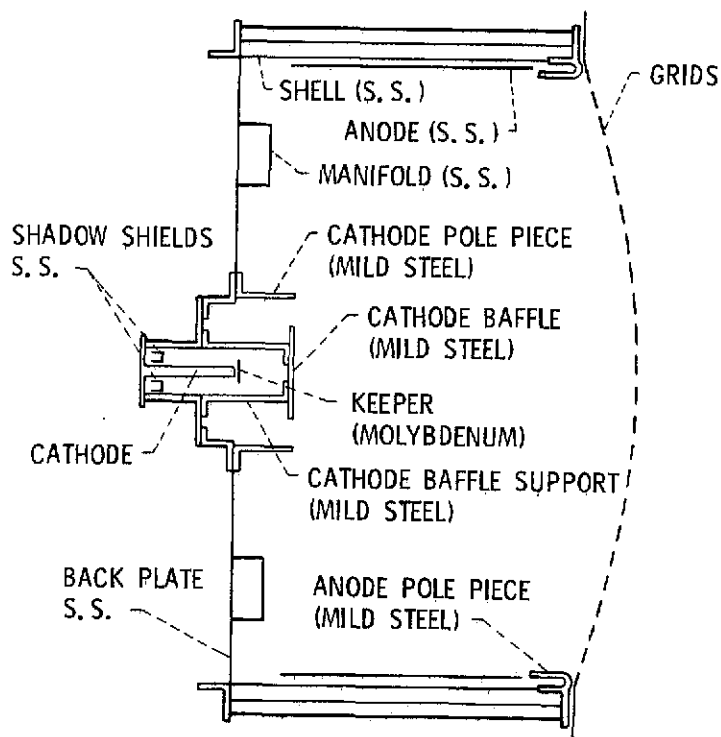
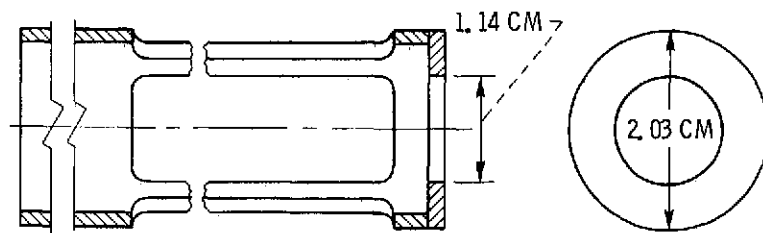
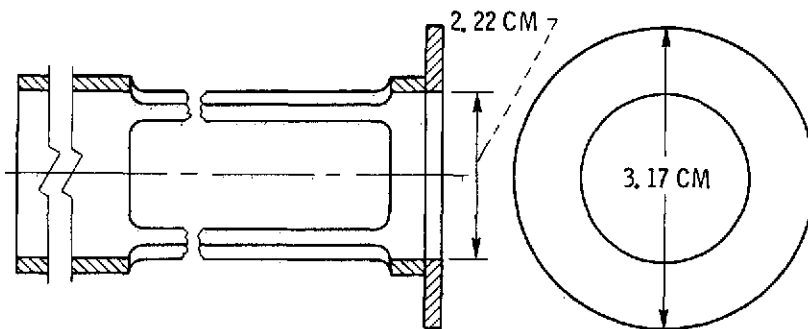


Figure 1. - Cross sectional view of a modified "400 series" thruster.

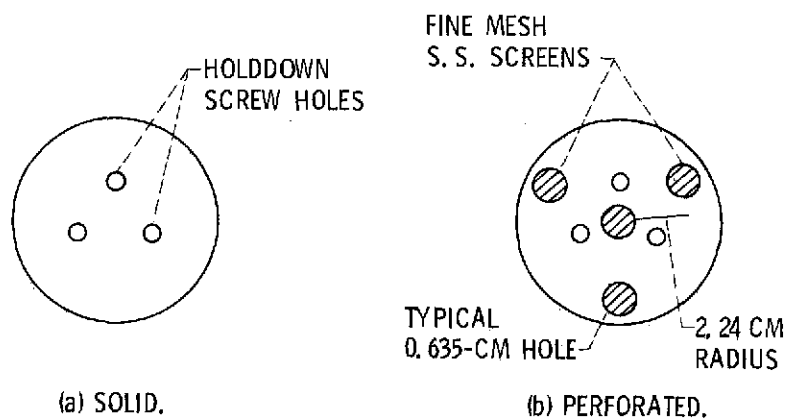


(a) "700 Series" baffle support.



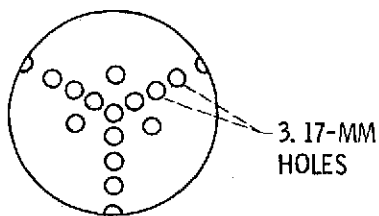
(b) "400 Series" baffle support.

Figure 2. - Baffle supports geometry of "400" and "700" series thrusters.



(a) SOLID.

(b) PERFORATED.



(c) MASKED.

Figure 3. - Cathode baffle geometries used in sputtering experiments.

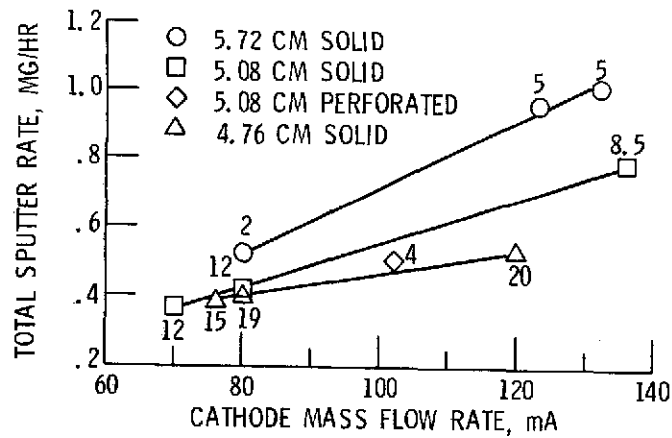


Figure 4. - Baffle sputtering rate of various baffles versus cathode mass flow rate. $J_B = 2.0$ A, $\Delta V_I = 37$ V, $\epsilon_I = 185$ eV/ion. Numbers next to data points indicate magnetic baffle current J_{MB} .

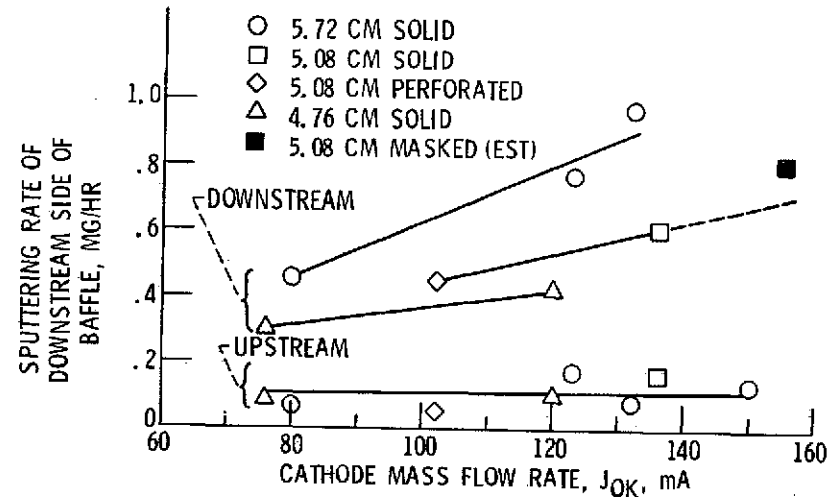


Figure 5. - Sputtering rates of upstream and downstream sides of various baffles versus cathode mass flow rate. $J_B = 2.0$ A, $\Delta V_I = 37$ V, $\epsilon_I = 185$ eV/ion.

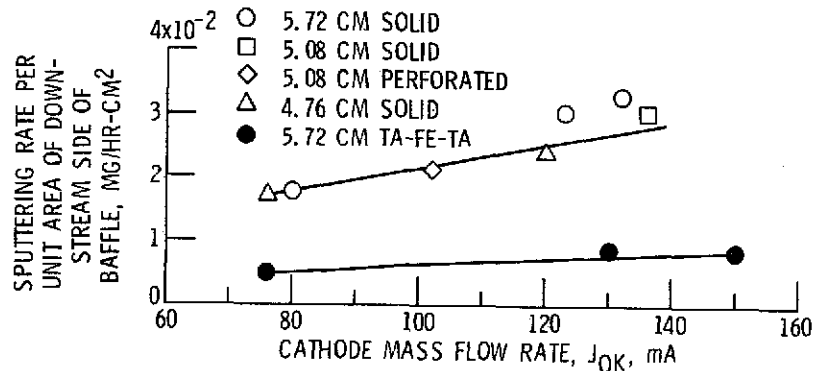


Figure 6. - Sputtering rates per unit area of various cathode baffles versus cathode mass flow rate. $J_B = 2.0$ A, $\Delta V_I = 37$ V, $\epsilon_I = 185$ eV/ion.

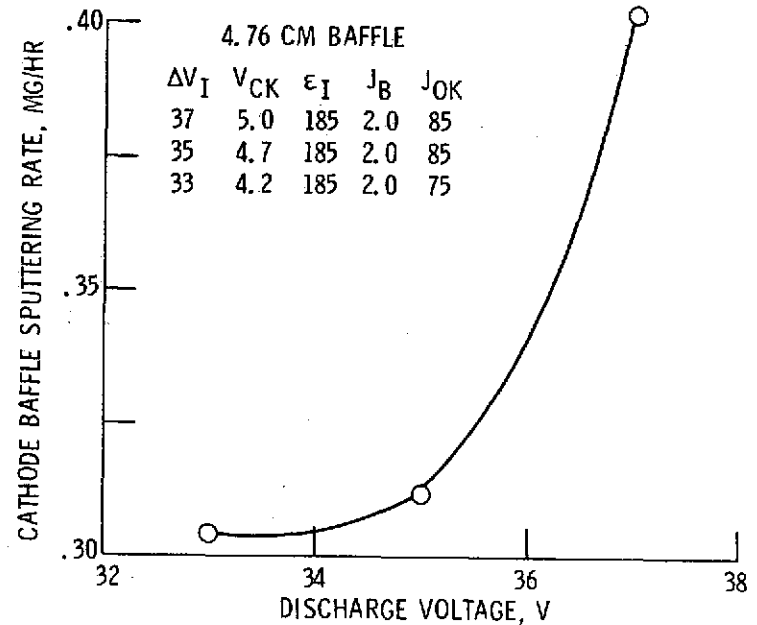


Figure 7. - Sputtering rates of baffle versus discharge voltage.

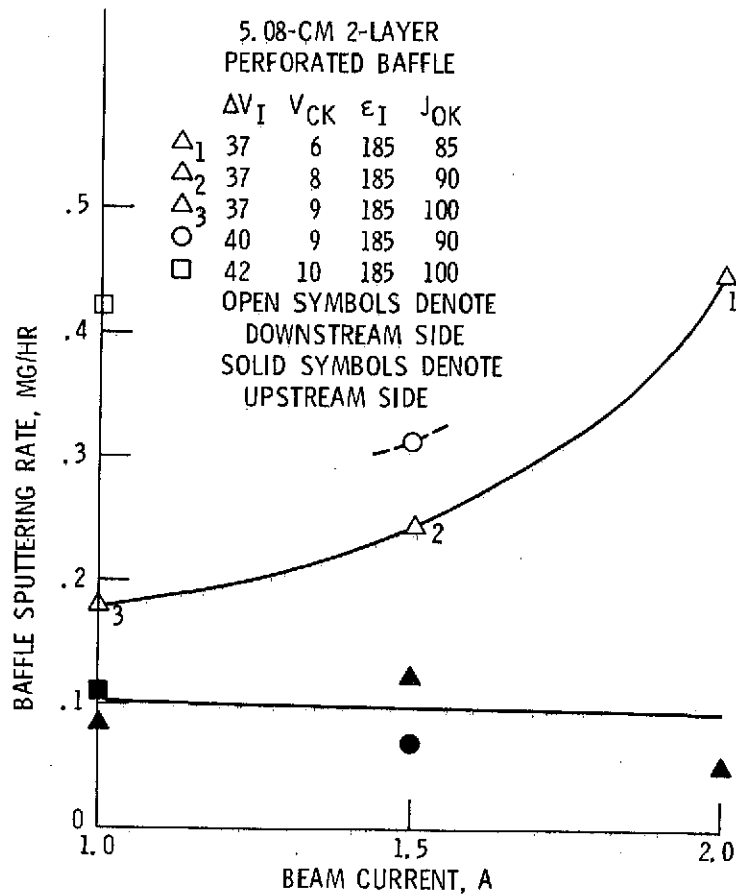


Figure 8. - Cathode baffle sputtering rate versus beam current.

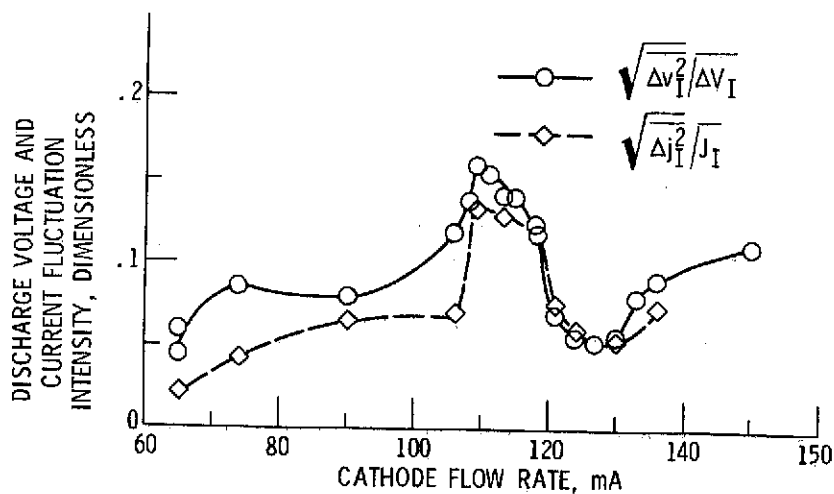


Figure 9. - RMS values of discharge voltage and current fluctuations versus cathode mass flow rate for a 5.08 cm iron baffle.

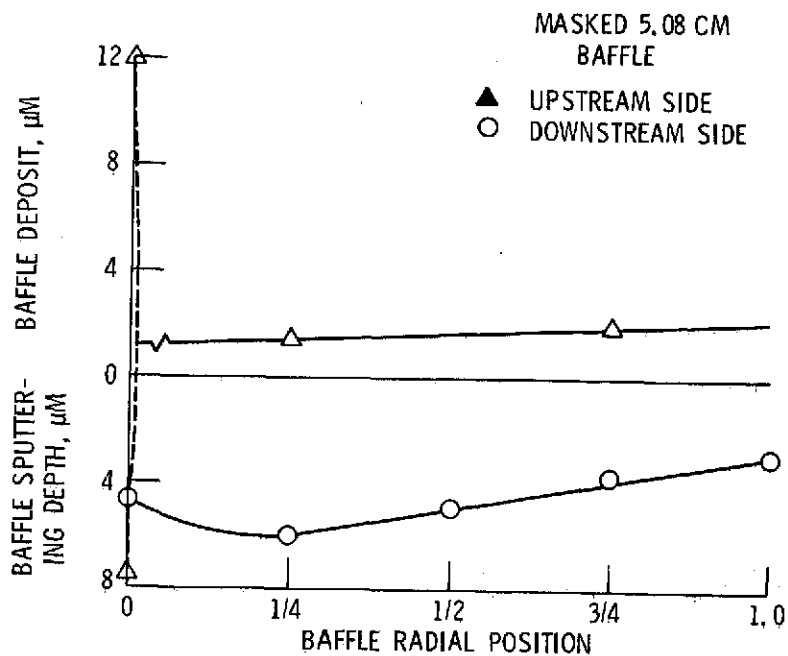
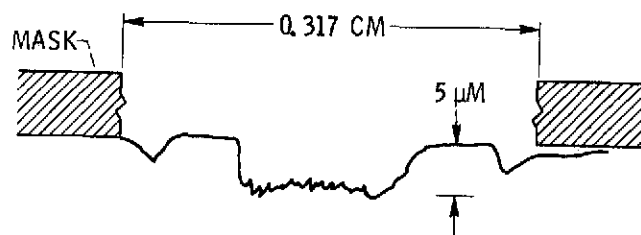


Figure 10. - Cathode baffle erosion and deposition in 75 hours versus baffle radial distance.



(a) CENTER HOLE, DOWNSTREAM SIDE.



(b) CENTER HOLE, UPSTREAM SIDE.



(c) DEPOSIT ON UPSTREAM SIDE OF BAFFLE, 3/4 RADIAL POSITION.

Figure 11. - Surface profileameter traces of masked baffle (75.5-hr test).

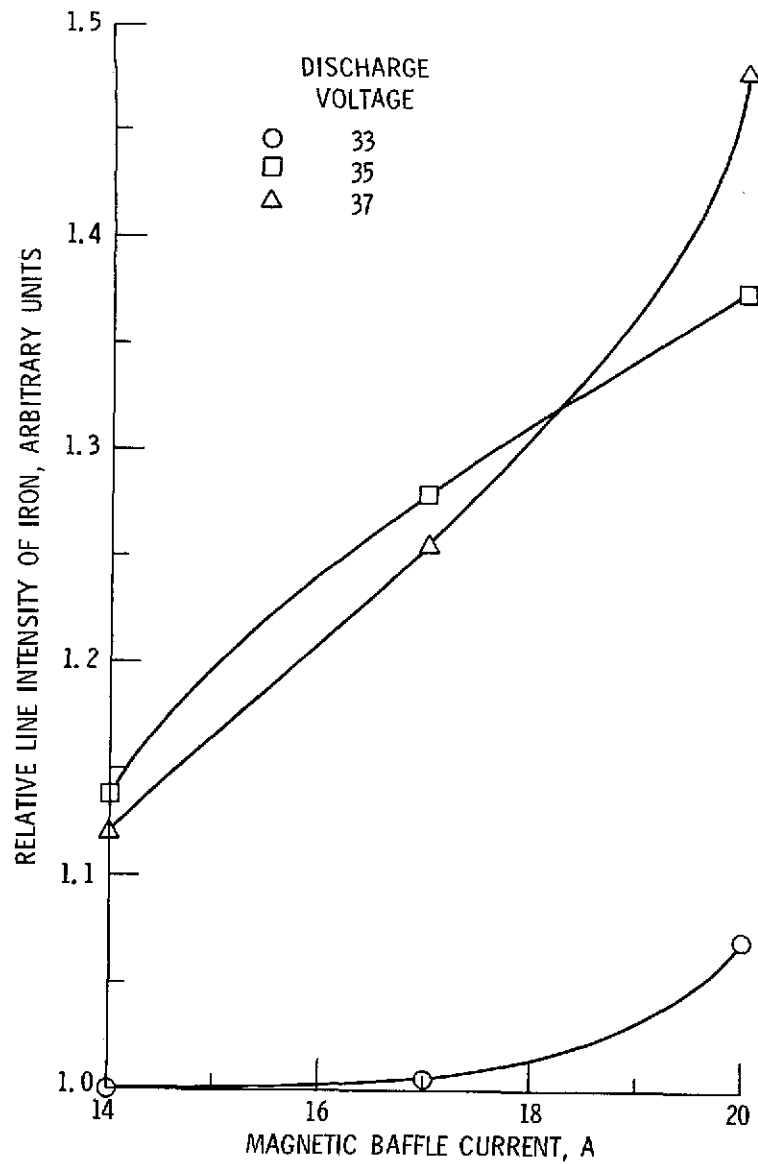


Figure 12. - Relative iron line (3720 Å) intensity versus magnetic baffle current. 4.76-cm baffle, $\epsilon_1 = 185$ eV/ion, $J_B = 2.0$ A.

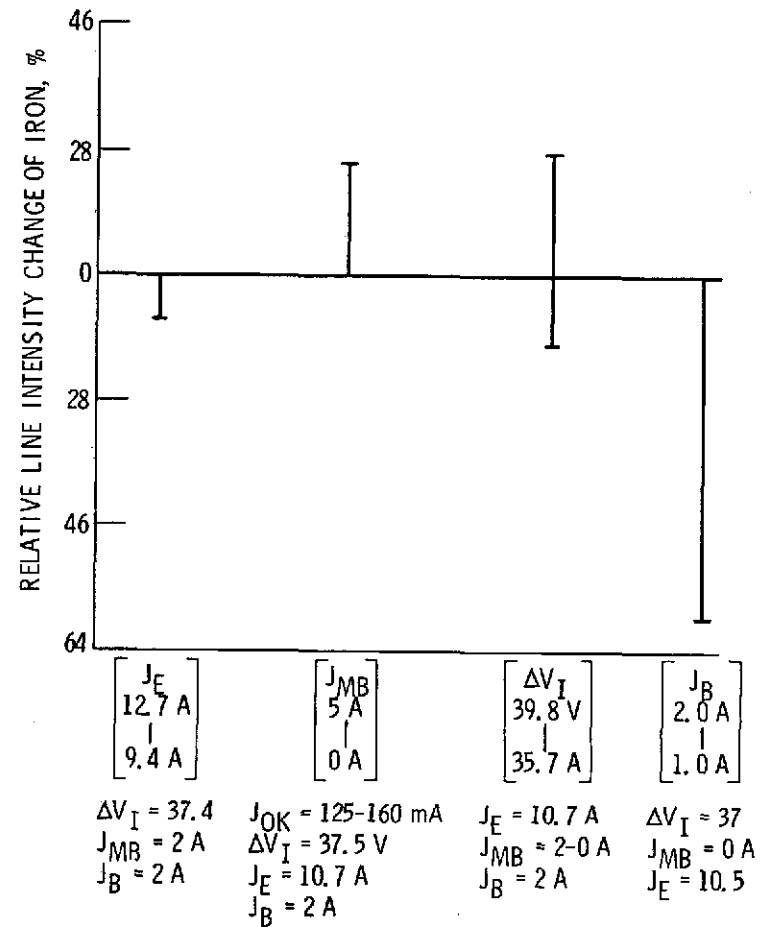


Figure 13. - Changes in relative intensity of Fe (3720 Å) from the normal thruster operating conditions as a function of thruster parameters. 5.72 cm Ta-Fe-Ta baffle.

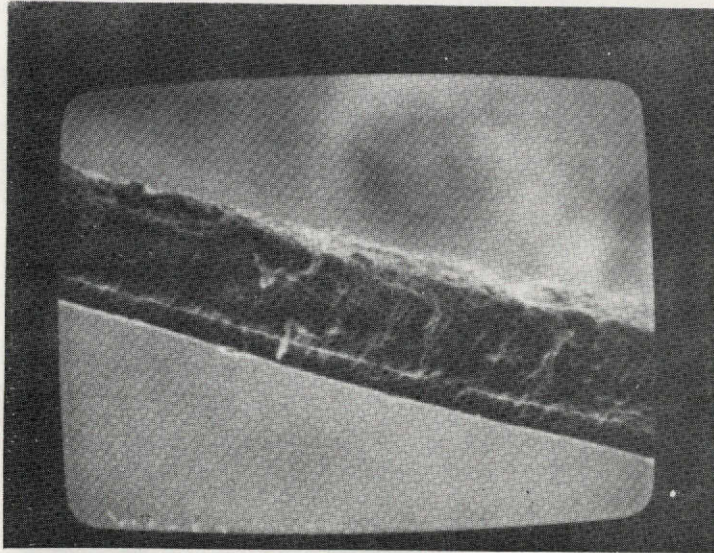


Figure 14. - Scanning electron microscope photograph of a sputtered material flake (20.5 microns thick) from anode.

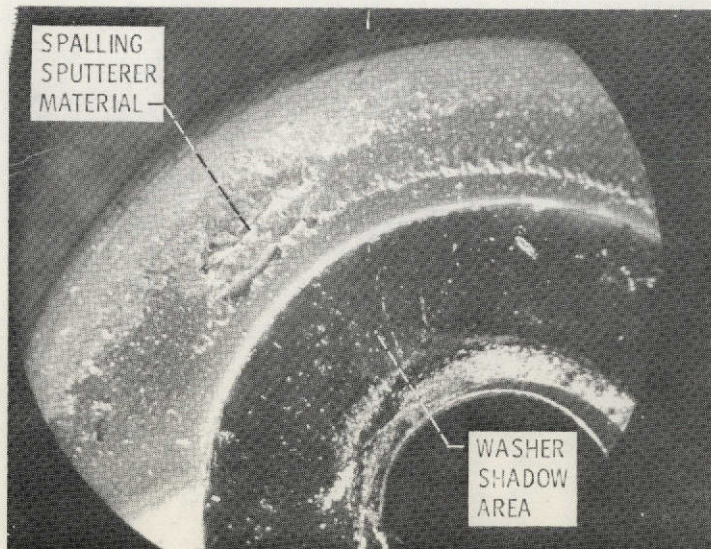


Figure 15. - Sputter deposited keeper shadow shield.